Supplement

Influence of NO_2 on secondary organic aerosol formation from ozonolysis of limonene

Changjin Hu[1,§], Qiao Ma[1,2,§], Zhi Liu[1], Yue Cheng[1], Liqing Hao[3], Nana Wei[1], Yanbo Gai[1], Xiaoxiao Lin[1], Xuejun Gu[1], Weixiong Zhao[1], Mingqiang Huang[1,4], Zhenya Wang[1], Weijun Zhang[1,2,5]

[1]Laboratory of Atmospheric Physico-Chemistry, Anhui Institute of Optics and Fine Mechanics, Chinese Academy of Sciences, Hefei 230031, Anhui, China

[2]University of Science and Technology of China, Hefei 230026, Anhui, China

[3]Department of Applied Physics, University of Eastern Finland, Kuopio 70211, Finland

[4]College of Chemistry & Environment, Minnan Normal University, Zhangzhou 363000, P. R. China

[5]School of Environmental Science and Optoelectronic Technology, University of Science and Technology of China, Hefei 230026, Anhui, China

§ These authors contributed equally to this work.

Correspondence to: Weijun Zhang (wjzhang@aiofm.ac.cn)

Chemicals.

(R)-(+)-limonene (97%) and 2-butanol (99.5%) were from Sigma-Aldrich Chemistry Corporation(Germany) and used directly without further purification. NO_2 (99.99%) was from Nanjing Special Gas Factory(China). Ozone was generated by passing purified ambient air (a mixture of N_2 and O_2) through a corona-discharge ozone generator (COM-AD-01-OEM, Anshan Anseros Environmental Protection Co., China). Relative humidity was controlled by passing a purified air stream through a 250-ml glass bulb with deionized water (conductivity 18.25 MΩ • cm@298K) in the chamber.

Experimental methods for off-line FTIR analysis

To investigate the chemical composition of SOA with FTIR analysis, when the diameter distribution of SOA tends to stabilization and the observed mass concentration comes to the top (about 1 hour after the initiation of the reaction in chamber), particle samples were drawn from the smog chamber through the filters (2.5 cm in diameter with a 0.5 μm pore size) at a rate of 3 L min^{-1} lasting for approximately 1 hour. Then the samples were analyzed with a FTIR spectrometer (Thermo Nicolet NEXUS) equipped with a Foundation Series horizontal attenuated total reflectance (ATR) accessory and a deuterated triglycine sulfate (DTGS) detector. The sample spectra in the range of 500-4000 cm^{-1} were obtained by placing the sampling filters directly onto the ATR crystal with 4 cm^{-1} resolution by averaging 32 scans. To ensure the clean background, the ATR crystal was completely cleaned between each sample spectrum acquisition, and an air background spectrum was also acquired.

Correction for SOA wall loss

Aerosol growth data should be corrected for wall loss, in which size-dependent coefficients determined from inert particle wall loss experiments are applied to the aerosol growth data (Keywood et al., 2004). According to the partitioning theory originally outlined by Pankow (Pankow, 1994a, b) and Odum et al (Odum et al., 1996), SOA yield is defined as the ratio of the amount of SOA formed to the amount of hydrocarbon consumed,

$$Y = \frac{\Delta M_0}{\Delta HC} \qquad (1)$$

where ΔM_0 ($\mu g/m^3$) is the mass of organic aerosol formed by the oxidation of ΔHC ($\mu g/m^3$).

Accurate determination of the SOA yield requires correction of wall losses. The wall loss of volatile hydrocarbon is negligible for FEP Teflon chamber. But for the aerosol, particle deposition onto the wall is significant as a result of turbulent, Brownian diffusion, gravitational sedimentation. Particle wall loss can be described as

$$\frac{dN(d_p)}{dt} = -k_{dep}(d_p)N(d_p) \qquad (2)$$

where $N(d_p)$ is the concentration of particles and $k_{dep}(d_p)$ is the deposition rate coefficient for particles with diameter d_p (Cocker et al., 2001). To determine the deposition rate of the aerosol and the wall loss of SOA in this chamber, decay of the nebulized ammonium sulfate aerosol was investigated as a substitute under the dark condition and at low particle concentration (~1000 particles cm^{-3}) in order to avoid the coagulation. The relationship between k_{dep} and d_p was determined by optimization of four parameters (a, b, c, and d) with the experimental data (Takekawa et al., 2003).

$$k_{dep}(d_p) = ad_p^b + c / d_p^d \qquad (3)$$

then $N(d_p)$ can be corrected and the suspended aerosol mass concentration ΔM_0 can be calculated from the wall-loss corrected volume concentration.

We also checked the wall loss by considering aerosol formation as a three-step process (Presto et al., 2005a)

$$oxidant(O_3) + VOC \xrightarrow{(k_0)} COC \qquad (R0)$$

$$COC \xrightarrow{(k_1)} \text{SOA} \qquad \text{(R1)}$$

$$SOA \xrightarrow{(k_2)} wall \qquad \text{(R2)}$$

Where COC stands for condensable organic carbon and wall loss is considered a terminal step. In this scenario, the analytical solution for SOA mass can be expressed as

$$SOA(t) = \frac{k_1 COC_0}{k_2 - k_1}(e^{-k_1 t} - e^{-k_2 t}) \qquad (4)$$

where COC_0 is the initial amount of condensable material formed by the oxidation reaction. Replacing ΔM_0 with COC_0 in eq 1 allows for extrapolation to an experiment that is free from wall loss.

Correction for SOA mass concentration is shown in Figure S1, where black squares are raw experimental data obtained from SMPS, red circles are corrected results according to the four-parameter method (Takekawa et al., 2003), while the red line shows the fit to the aerosol mass data according to eq 4 and the y-intercept of the dashed line illustrates the corresponding wall-loss correction (COC_0) (Presto et al., 2005). In the four-parameter method, the value of ΔM_0 used in eq 1 can be determined when the suspended aerosol mass concentration (corrected for wall losses) become steady. Whereas in the three-step process, the initial amount of condensable material formed COC_0 can be determined by extrapolation back to t=0 according to eq 4, namely the y-intercept of the dashed line. It can be found from Figure S1 that the two correction methods agree with each other very well in this work, and the relative error between the two scenarios is about 5%, which validated the results presented in the work. The former, however, was mainly used in this work.

References

Cocker, D. R., Flagan, R. C., and Seinfeld, J.H.: State-of-the-art chamber facility for studying atmospheric aerosol chemistry. Environ. Sci. Technol., 35, 2594–2601, 2001.

Donahue, N. M., Tischuk, J. E., Marquis, B. J. and Huff Hartz, K. E.: Secondary organic aerosol from limona ketone: insights into terpene ozonolysis via synthesis of key intermediates, Phys. Chem. Chem. Phys., 9, 2991–2998, 2007.

Keywood, M. D., Varutbangkul, V., Bahreini, R., Flagan, R. C., and Seinfeld, J.H.: Secondary organic aerosol formation from the ozonolysis of cycloalkenes and related compounds. Environ. Sci. Technol., 38, 4157–4164, 2004.

Odum, J. R., Hoffmann, T., Bowman, F., Collins, D., Flagan, R. C., and Seinfeld, J. H.: Gas/Particle Partitioning and Secondary Organic Aerosol Yields. Environ. Sci. Technol., 30, 2580–2585, 1996.

Pankow, J. F.: An absorption model of the gas/aerosol partitioning of organic compounds in the atmosphere. Atmos. Environ., 28, 185–188,1994a.

Pankow, J. F.: An absorption model of the gas/aerosol partitioning involved in the formation of secondary organic aerosol. Atmos. Environ., 28, 189-193, 1994b.

Presto, A. A., Hartz, K. E. H., and Donahue, N. M.: Secondary organic aerosol production from terpene ozonolysis. 1. Effect of UV radiation. Environ. Sci. Technol., 39, 7036−7045, 2005.

Takekawa, H., Minoura, H., and Yamazaki, S.: Temperature dependence of secondary organic aerosol formation by photo-oxidation of hydrocarbons. Atmos. Environ., 37, 3413–3424, 2003.

Zhang, J. Y., Huff Hartz, K. E., Pandis S. N., and Donahue, N. M.: Secondary organic aerosol formation from limonene ozonolysis: Homogeneous and heterogeneous influences as a function of NO_x, J. Phys. Chem. A, 110, 11053–11063, 2006.

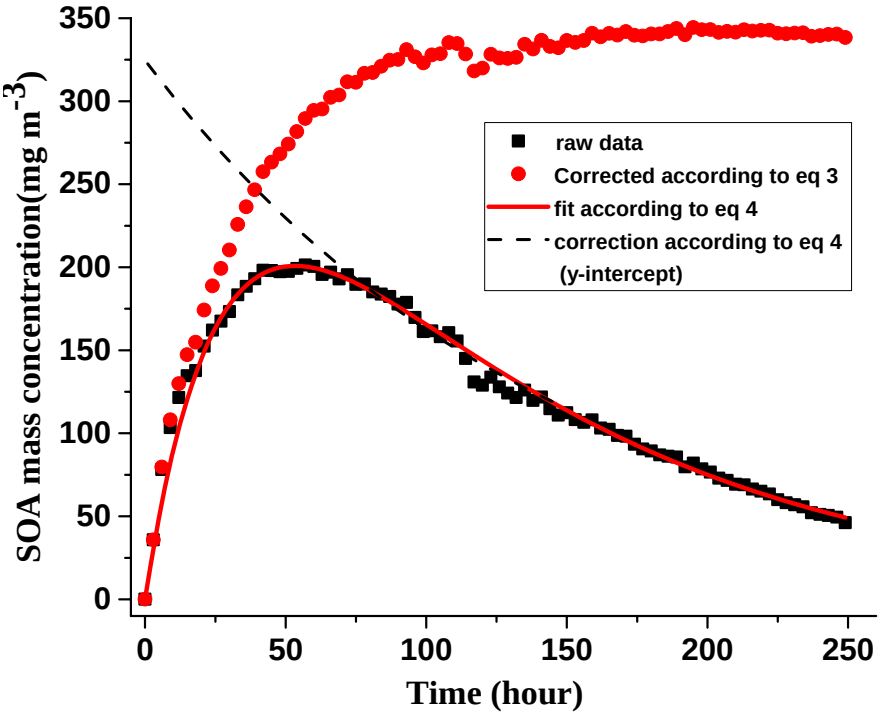

Figure S1. Correction for SOA mass concentration. Black squares represent experimental data (Exp. N19 in Table 1), red circles are corrected results according to the four-parameter method, and the red line shows the fit to SOA mass concentration according to eq 4.

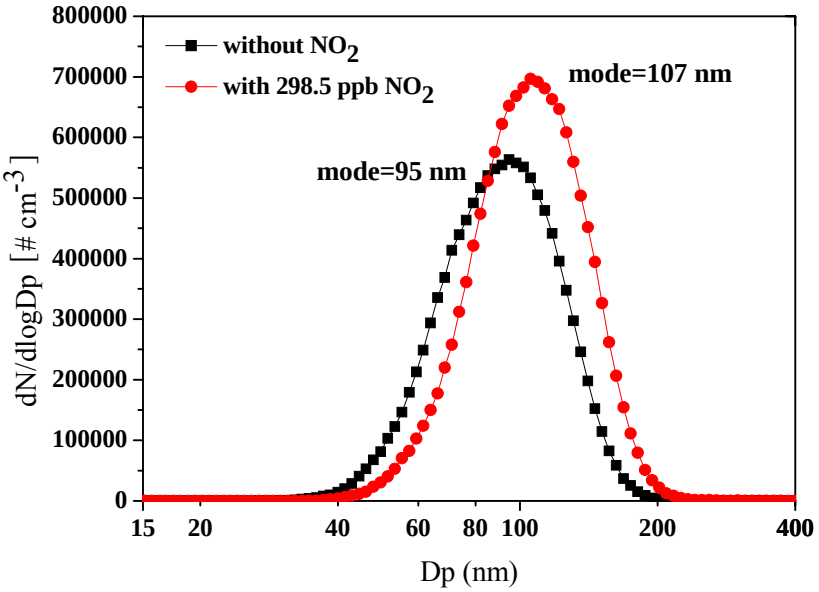

Figure S2. The effect of 298.5 ppbv NO_2 on the particle size distribution of SOA formation from limonene ozonolysis after 60 min of reaction (raw data).

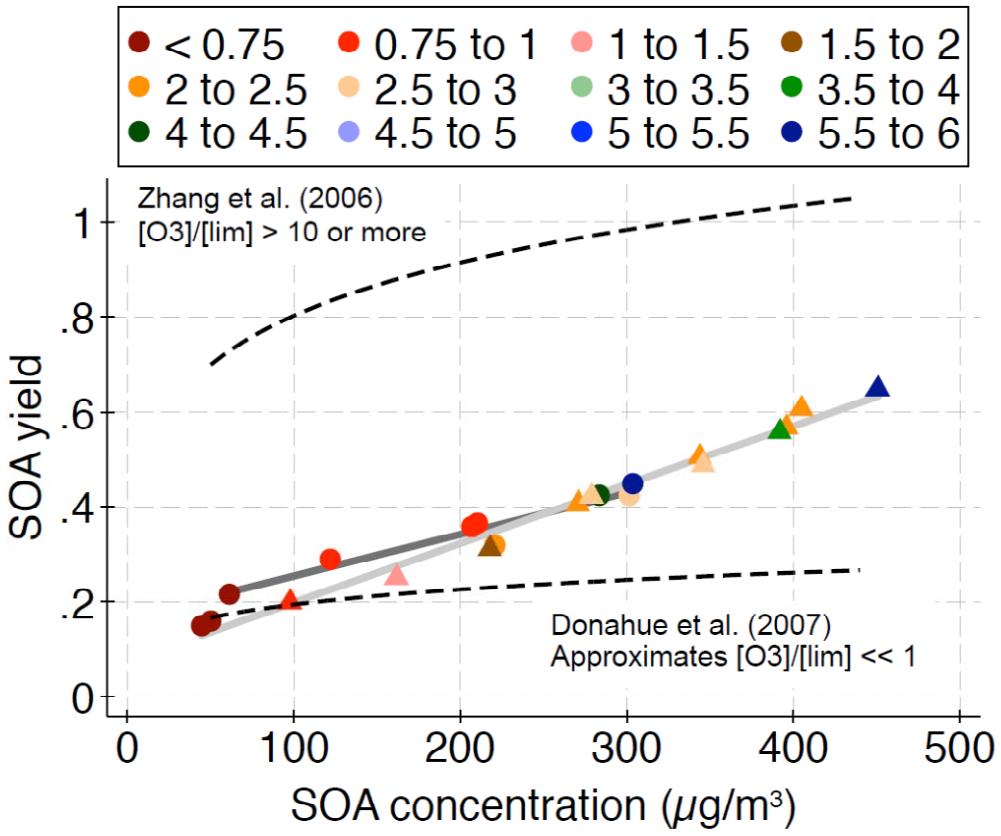

Figure S3. Comparison of the SOA yield in this work with those in reference. (The two dashed line represent fits to yields from Zhang et al.2006 and Donahue et al. 2007 respectively. The dots (without NO_2) and the triangle (with NO_2) are experiment data of this work, and the different colour represents different ozone-to-limonene ratio)

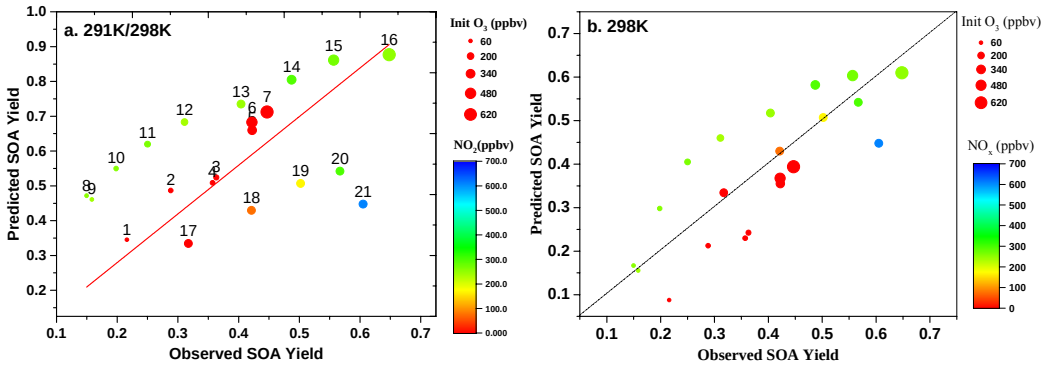

Figure S4. Comparison of the fitting under the different temperatures (a, N1-N16 at 291K and N17-N21 at 298K, the slope of the line is 1.40 ; b, all N1-N21 at 298K, the slope of the line is 1.0)

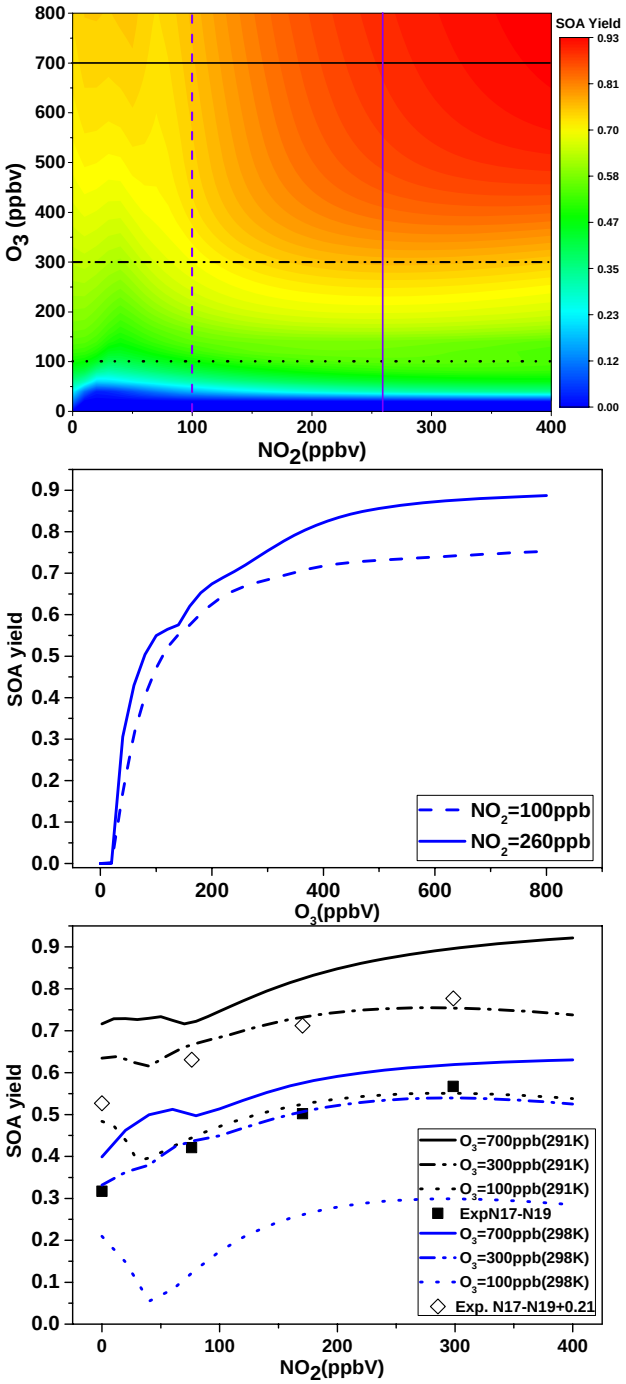

Figure S5. (a)Organic aerosol yield as a function of the initial concentrations of O_3 and NO_2. (b) SOA yield as a function of the initial concentrations of O_3 at the two represented NO_2 concentrations, which correspond to the two vertical lines shown in (a). (c) SOA yield as a function of the initial concentrations of NO_2 at the three represented O_3 concentrations, which correspond to the three horizontal lines shown in (a).(■ stands for experimental data of N17-N19, ◇ stands for experimental data of N17-N19 plus 0.21)

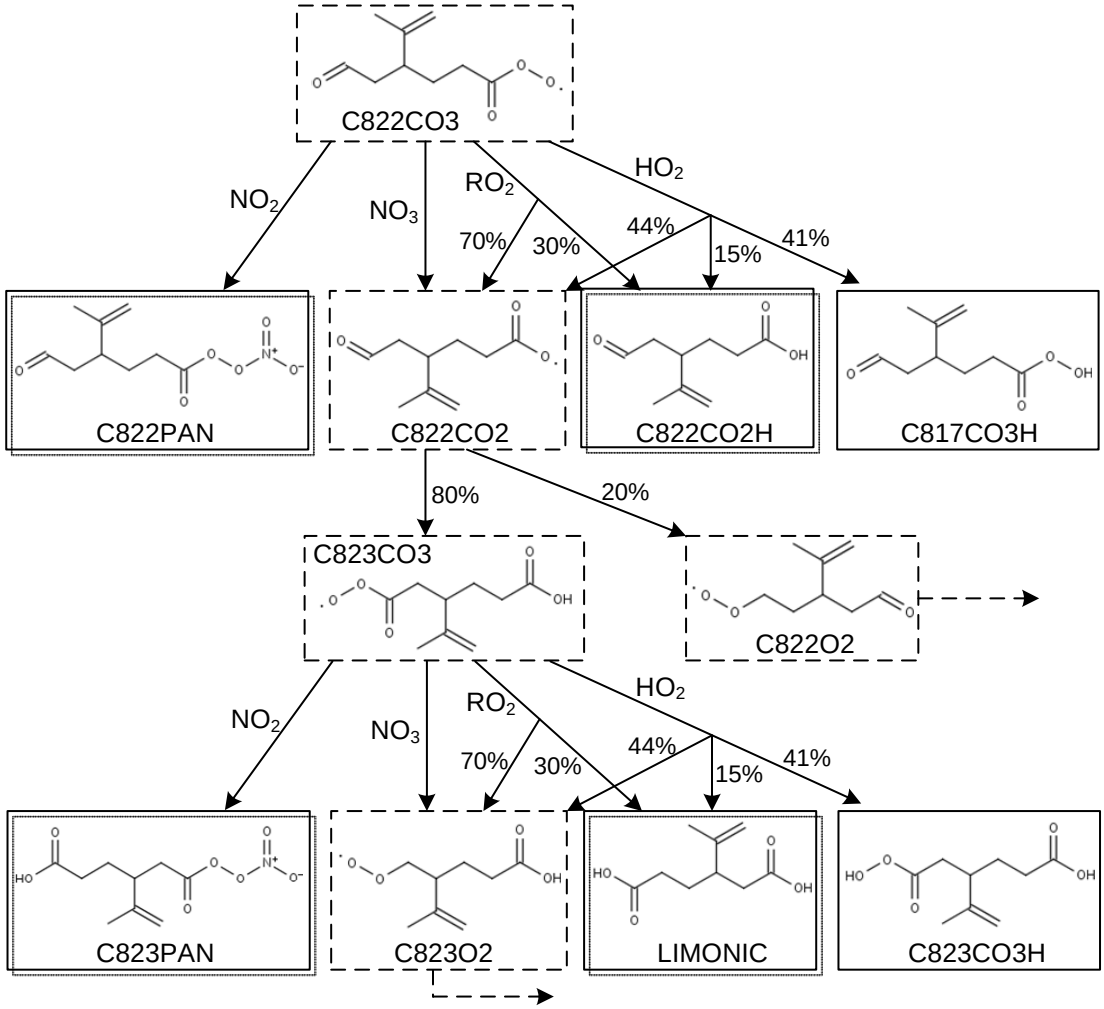

Scheme S1. Partial schematic of the degradation mechanism for one of the secondary-generation peroxy radicals, C822CO3. (The symbols here have the same meanings to that in Scheme 1).

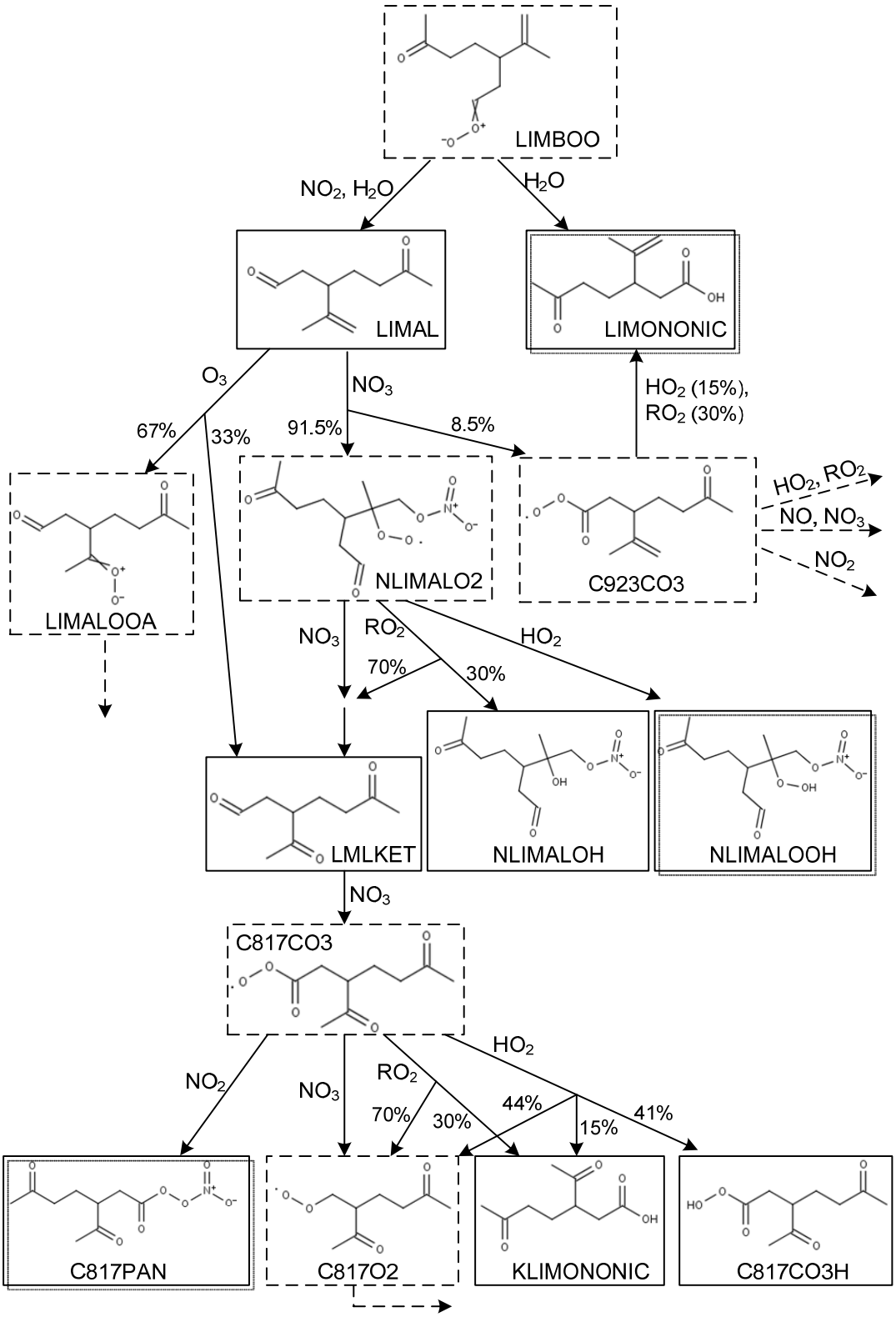

Scheme S2. Partial schematic of the degradation mechanism for one of the major stable Criegee intermediate, LIMBOO.